Reversible Phosphorylation Subserves Robust Circadian Rhythms by Creating a Switch in Inactivating the Positive Element

Zhang Cheng, Feng Liu,* Xiao-Peng Zhang, and Wei Wang*
National Laboratory of Solid State Microstructures and Department of Physics, Nanjing University, Nanjing, China

ABSTRACT Reversible phosphorylation of proteins is ubiquitous in circadian systems, but the role it plays in generating rhythmicity is not completely understood. A common mechanism for most circadian rhythms involves a negative feedback loop between the positive and negative elements. Here, we built a minimal model for the *Neurospora crassa* circadian clock based on the core negative feedback loop and the protein FREQUENCY (FRQ)-dependent phosphorylation of the White Collar Complex (WCC). The model can reproduce basic features of the clock, such as the period length, phase relationship, and entrainment to light/dark cycles. We found that the activity of WCC can be controlled by FRQ in a switchlike manner owing to zero-order ultrasensitivity. WCC is inactivated when FRQ level crosses a threshold from below. As a result, low cooperativity in transcriptional activation is sufficient for circadian rhythms, and the level of active WCC exhibits spiky oscillations. Such oscillations are robust to molecular noise and may subserve controlling circadian output. Therefore, the core negative feedback together with phosphorylation of the positive element can ensure robust circadian rhythms. Our work provides insights into the critical roles of posttranslational modification in circadian clocks.

INTRODUCTION

Circadian clocks are self-sustained cellular oscillators that control a wide variety of daily biochemical, physiological, or behavioral processes (1–3). A common molecular mechanism underlying most circadian rhythms engages a negative transcriptional/translational feedback loop between a positive and a negative element (1). The positive element is usually a transcription activator inducing expression of the negative element, whereas the negative element inhibits transactivity of the positive element via various mechanisms (1).

The filamentous fungus *Neurospora crassa* is a premier model organism for studying circadian clocks because of its simplicity and overall similarity to the animal circadian systems (4–6). In the core circadian oscillator of *N. crassa*, the transcription factors White Collar-1 (WC-1) and White Collar-2 (WC-2) assemble, forming the White Collar Complex (WCC), which induces expression of the *frequency* (*frq*) gene (7,8). The protein FREQUENCY (FRQ) then inhibits its own synthesis by repressing the activity of WCC, closing the feedback loop (9–12). That is, WCC and FRQ are separately the positive and the negative element. Note that FRQ, WC-1, and WC-2 can all be modulated by phosphorylation effects (for review, see (13)), and such phosphorylation is essential for retaining circadian rhythms. Although the negative feedback structure is identified, how FRQ inhibits WCC is still hotly debated.

It was previously thought that FRQ represses WCC by direct binding and by dissociating it from the *frq* promoter (11,12), on which some theoretical models were based (14,15). However, this mechanism was questioned by the new evidence that in the nucleus, FRQ level is much lower than WCC level and only a small fraction of WCC is in complex with FRQ (16). Thus, the possibility of 1:1 binding to WCC and sequestering WCC by FRQ was excluded. Instead, it was suggested that FRQ regulates the activity of WCC through modulating its phosphorylation status. FRQ may act like a scaffold protein transiently recruiting one or more kinases (CKI and CKII) to phosphorylate WCC (16,17). Clearly, WCC in its hyperphosphorylated state exhibits a lower affinity for binding to the Clock(C)-box in the *frq* promoter and is less active in driving *frq* transcription than hypophosphorylated WCC (16). However, it is unclear how such FRQ-dependent phosphorylation of WCC contributes to circadian rhythms.

Moreover, reversible phosphorylation of proteins also regulates other important processes involved in various circadian clocks, such as nuclear entry, formation of protein complexes, and protein degradation (18). In particular, it was found that the cyanobacteria can maintain circadian rhythms by phosphorylation of clock proteins in the absence of transcription-translation feedback (19,20). Thus, exploring the role of posttranslational modification in circadian clocks will provide new insights into the mechanisms for various circadian rhythms.

Motivated by the above considerations, here we aim to explore the kinetics of FRQ-dependent phosphorylation of WCC and its role in generating sustained oscillations. We construct a minimal model for the *N. crassa* circadian clock, involving the core negative feedback loop closed by FRQ-dependent phosphorylation of WCC. The model is able to mimic salient characteristics of the clock, such as the period length, phase differences between clock components, and the entrainment to light/dark cycles. When the reversible phosphorylation reactions operate near saturation, there exists

Submitted July 13, 2009, and accepted for publication September 3, 2009.

*Correspondence: fliu@nju.edu.cn or wangwei@nju.edu.cn

Editor: Andre Levchenko.

0006-3495/09/12/2867/9 $2.00

doi: 10.1016/j.bpj.2009.09.008

a dynamic switch for the level of active WCC controlled by FRQ level, such that WCC is efficiently repressed by FRQ. Consequently, low cooperativity in inducing *frq* transcription is sufficient for circadian rhythms, and spiky oscillations in the level of active WCC are generated, which makes the oscillator robust to intrinsic noise and subserves mediating the expression of downstream clock-controlled genes. Thus, our results suggest that the phosphorylation of clock elements is important for ensuring robust circadian rhythms. We also compare our model with previous models and propose experiments to probe the hypothesis presented here.

MODEL AND METHODS

The model is depicted in Fig. 1. Here, we consider only two distinct phosphorylation states of WCC, the hypophosphorylated and hyperphosphorylated WCC, as in Schafmeier et al. (16). The hypophosphorylated WCC (WCC*) is active, inducing expression of *frq*. After FRQ protein is synthesized, the protein kinases CKI and CKII are recruited to phosphorylate WCC*, which then becomes inactive and is disassociated from the *frq* promoter (16,17). After the amount of FRQ drops to a low level, the hyperphosphorylated WCC (WCC_P) is dephosphorylated by the phosphatase PP2A, which results in the activation of WCC and *frq* transcription in a new cycle (16).

The rate equations of the model are written as

$$\frac{dx_1}{dt} = k_1\frac{x_3^n}{x_3^n + K_1^n} - k_2x_1, \quad (1)$$

$$\frac{dx_2}{dt} = k_3x_1 - k_4x_2, \quad (2)$$

$$\frac{dx_3}{dt} = k_5\frac{x_{3P}}{x_{3P} + K_2} - k_6x_2\frac{x_3}{x_3 + K_3}, \quad (3)$$

where x_1, x_2, x_3, and x_{3P} denote the concentrations of *frq* mRNA, FRQ protein, WCC*, and WCC_P, respectively. Note that the total WCC level is supposed to be constant, i.e., $x_3 + x_{3P} = constant$ (see below for details).

The activation of *frq* transcription is characterized by Hill function with coefficient n. The enzymatic reactions are described by the Michaelis-Menten function. To mimic the FRQ-dependent phosphorylation of WCC, the maximum phosphorylation rate is assumed to be proportional to FRQ level. For the sake of simplicity, the degradation of *frq* mRNA and FRQ is modeled as first-order reactions, and the Michaelis constants for CKI/II- and PP2A-catalyzed reactions are assumed to be identical, i.e., $K_2 = K_3$.

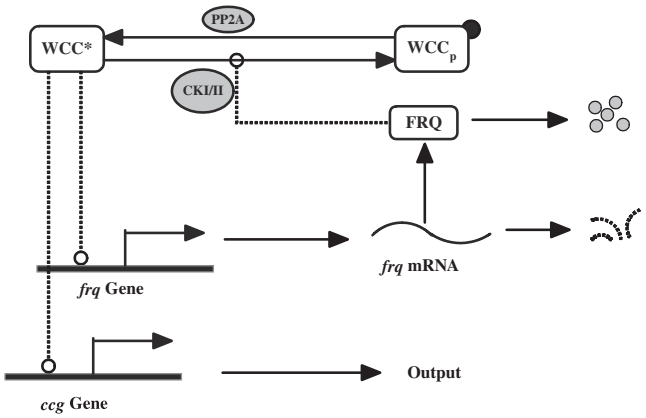

FIGURE 1 Schematic depiction of the model. The transcription factor WCC activates the *frq* transcription, whereas FRQ protein suppresses the activity of WCC by promoting its phosphorylation. The phosphorylation and dephosphorylation of WCC are separately catalyzed by the kinase CKI/II and the phosphatase PP2A.

Several other assumptions are made to simplify the model and to facilitate the discussion on the role of reversible phosphorylation. First, a positive feedback loop in which FRQ supports accumulation of WCC is not included here (21,22). Second, the total WCC level (i.e., $[WCC]_t = [WCC^*] + [WCC_P]$) is assumed to be constant because it oscillates with a low amplitude compared with FRQ level (21,22). Third, the production and degradation of WCC are ignored.

To quantify the overall degree of saturation for an enzymatic reaction, we define its Michaelis constant divided by the total level of substrate as a relative Michaelis constant. The ratio of K_2 to $[WCC]_t$ is denoted by k_m. When saturated (i.e., $[WCC]_t >> K_2$), most enzymes form complexes with the substrate, and the reaction rate is independent of the abundance of substrate (23).

In the *N. crassa* circadian clock, the degradation rate of FRQ is usually a key parameter because it sets the dynamical timescale of the system (24). Since the half-life of FRQ is 4 ~ 7 h, k_4 is set to 0.14 h^{-1} (25). The other standard parameters used are as follows: $k_1 = 10$ nM h^{-1}, $k_2 = 0.17$ h^{-1}, $k_3 = 1$ h^{-1}, $k_5 = 9$ nM h^{-1}, $k_6 = 1$ h^{-1}, $K_1 = 5$ nM, $K_2 = 0.1$ nM, $K_3 = 0.1$ nM, $[WCC]_t = 10$ nM, and $n = 5$. Accordingly, $k_m = 0.01$. Integration of differential equations is performed using a fourth-order Runge-Kutta method with a time step of 0.01 h.

Moreover, since chemical reactions are essentially probabilistic and reactants such as mRNA and proteins are present in low numbers per cell, intrinsic noise is inevitable. We also build the stochastic version of the model, which generally can be described by birth-and-death stochastic processes governed by chemical master equations. We use the Gillespie method to simulate the master equations (26). By introducing a system size factor Ω, we change the concentrations x_i of clock components to the numbers X_i of molecules, i.e., $X_i = \Omega x_i$. The reactions involved are listed in Table 1. Note that the total number of WCC is constant, namely $X_3 + X_{3P} = \Omega[WCC]_t$.

RESULTS

Modeling basic features of the *N. crassa* circadian clock

Fig. 2 *A* exhibits the oscillations of *frq* mRNA, FRQ protein, and WCC* levels. The oscillation period is 22.03 h, consistent with experimental measurements in the wild-type (frq^+) strain under constant darkness (22 h at 25°C) (9). The phase lag between the peak levels of *frq* mRNA and FRQ is 4.67 h, in agreement with the experimental value of

TABLE 1 Stochastic transition processes and the corresponding transition rates

No.	Transition process	Description	Transition rate
1.	$X_1 \rightarrow X_1 + 1$	The transcription of *frq* activated by WCC*	$\Omega k_1\frac{X_3^n}{X_3^n + (K_1\Omega)^n}$
2.	$X_1 \rightarrow X_1 - 1$	The degradation of *frq* mRNA	k_2X_1
3.	$X_2 \rightarrow X_2 + 1$	The synthesis of FRQ protein	k_3X_1
4.	$X_2 \rightarrow X_2 - 1$	The degradation of FRQ protein	k_4X_2
5.	$X_3 \rightarrow X_3 + 1$	The dephosphorylation of WCC_P by PP2A	$\Omega k_5\frac{X_{3P}}{X_{3P} + K_2\Omega}$
6.	$X_3 \rightarrow X_3 - 1$	The phosphorylation of WCC* promoted by FRQ	$k_6X_2\frac{X_3}{X_3 + K_2\Omega}$

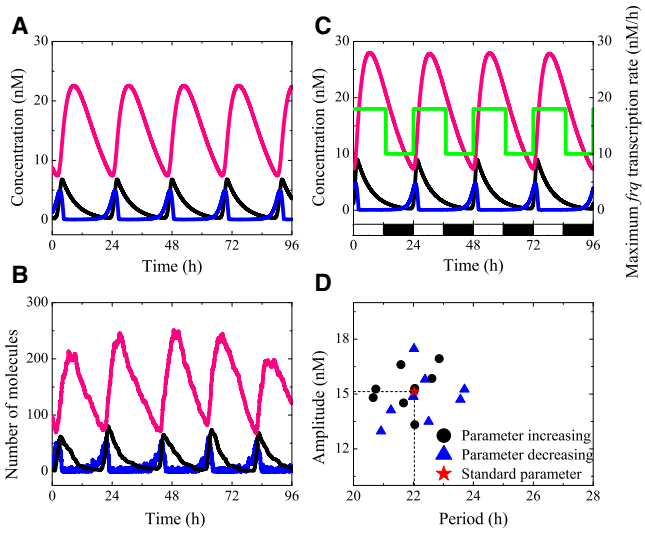

FIGURE 2 Robust circadian oscillations. Temporal evolution of the levels of *frq* mRNA (*black line*), FRQ protein (*pink line*), and WCC* (*blue line*) in the absence (*A*) or presence (*B*) of intrinsic noise or in response to light/dark cycles without noise (*C*) (color online only). Green line in panel *C* shows the time course of the maximum *frq* transcription rate k_1. (*D*) Period and amplitude of oscillations of FRQ level when each of nine parameters is increased or decreased by 15% with respect to the standard parameter set. Clearly, the clock is robust to variations in parameter values.

4 ~ 6 h (27). Over one circadian cycle, the inhibition phase in which FRQ represses its own synthesis lasts ~3.12 h, whereas the recovery phase in which the repression is released and the amount of *frq* transcript returns to a high level lasts ~18.91 h. The length of both the two phases agrees well with the experimental measurements (28). Furthermore, when intrinsic noise is added to the model with $\Omega = 10$, the rhythmicity can be well kept though the amplitudes of oscillations are variable (Fig. 2 *B*).

One important feature of the oscillator is the pulselike oscillation of WCC* level. To characterize the spikiness of oscillations, we use a similar measure to that in Krishna et al. (29), namely $Z_i = (\max(C_i) - \min(C_i))/(\text{mean}(C_i) - \min(C_i))$, with C_i denoting the concentration of clock-component. Generally, oscillations are termed spiky when $Z > 2$, and soft otherwise (29). Here, the Z values are 5.93, 2.98, and 0.97 for the oscillations of [WCC*], [*frq*] and [FRQ], respectively, in the absence of noise. Therefore, the oscillations of [WCC*] and [*frq*] are spiky, whereas the oscillations of [FRQ] are more smooth (Fig. 2 *A*). The mechanism for the spiky oscillation of [WCC*] is revealed later, and its significance is explored in the Summary and Discussion.

Entrainment to a 12:12 light/dark cycle is also manifest in our model. The effect of light is introduced by making the maximum transcription rate k_1 light-sensitive, which is realized in our simulations by setting $k_1 = 18$ nM h^{-1} with light and $k_1 = 10$ nM h^{-1} otherwise. This is consistent with the experimental observation that light can increase the transcription rate of *frq* (30), and a similar assumption has been made in Leloup et al. (31). Fig. 2 *C* indicates that the oscillator is entrained precisely to the external period of 24 h, which is characteristic of the *N. crassa* circadian clock.

We also vary the parameter values to see whether the circadian rhythm is still stable (14,15). For each case, only one of nine model parameters is increased or decreased by 15% with respect to the standard parameter set. Together with the standard parameter set, there are 19 sets of parameter values. The period and amplitude of oscillations in FRQ level for different parameter values are plotted in Fig. 2 *D*, where the dots are nearly uniformly distributed. Table 2 lists the percentage of changes in the period and amplitude. Compared to the case with the standard parameter set, the period length changes by <8% whereas the amplitude varies by <16%. Moreover, even when the parameter values are changed by 50%, no oscillations are lost. These indicate that the circadian rhythm produced in our model is stable against parameter variations.

Clearly, the period is most sensitive to the degradation rates of *frq* mRNA and FRQ, k_2 and k_4, whereas the amplitude is most sensitive to the maximum rate constant of phosphorylation, k_6, and the Hill coefficient n (see Table 2). In particular, the period length increases (or decreases) with decreasing (increasing) the degradation rates of FRQ and/or *frq* mRNA. For example, the period length rises to 29 h when k_2 is decreased by 50%. Interestingly, the period length also rises to ~29 h in the frq^7 mutant with the amino-acid substitution of Gly-459 to Asp, which results in a slower degradation rate (32,33). In contrast, the period length drops to 18 h when k_2 is increased by 50%; this is consistent with the experimental observation in the frq^2 mutant with Ala-895 converted to Thr (32,33). It would be helpful to experimentally measure the relationship between the degradation rates or half-life of different FRQ mutants and the period length. This will subserve setting parameter values in modeling so that precise predictions can be made.

Since the reversible phosphorylation of WCC is included in our model, it is possible to study the effects of mutation in

TABLE 2 Percentage of changes in the period (*P*) and amplitude (*A*) of oscillations in FRQ level compared to the case with the standard parameter set

	+15%		−15%		+50%		−50%	
Parameter	*P* (%)	*A* (%)	*P* (%)	*A* (%)	*P* (%)	*A* (%)	*P* (%)	*A* (%)
k_1	0.07	1.3	−0.2	−1.8	0.03	3.1	−1.3	−10.0
k_2	**−6.3**	−2.1	**7.6**	0.8	**−17.4**	−8.6	**33.3**	−10.1
k_3	0.07	1.3	−0.2	−1.9	0.02	3.13	−1.3	−10.1
k_4	**−5.8**	0.9	**7.0**	−2.8	**−16.4**	−1.0	**28.9**	−23.8
k_5	−2.0	9.6	2.2	−10.8	−6.1	28.8	8.6	−41.3
k_6	0.07	**−11.9**	−0.2	**15.3**	0.03	**−31.2**	−1.3	**80.0**
K_1	2.7	4.8	−3.5	−6.7	6.9	10.6	−18.5	−35.5
k_m	−1.6	−4.2	1.6	4.4	−5.0	−12.8	5.9	16.5
n	3.72	**11.8**	−5.0	**−14.3**	9.6	**33.1**	−32.5	**−68.4**

For each case, the value of one of nine parameters is increased or decreased by 15% or 50% with respect to the standard parameter set. The bolded values in each column indicate that the period or the amplitude is most sensitive to variation in the corresponding parameters.

the kinase and phosphatase on circadian rhythms. For example, when the rate constant of dephosphorylation, k_5, is reduced, the period length increases but the amplitude decreases. This is consistent with the experimental observation in the rgb^{RIP} mutant, in which RGB-1 (a regulatory subunit of PP2A) is disrupted by repeat-induced point mutation (RIP) (34,35). The mutation evokes a reduced phosphatase activity leading to a lower-amplitude and longer-period oscillation (35).

Furthermore, we perform parameter sensitivity analysis (36) to systematically explore how the oscillator is sensitive to variation in each parameter. Parameter sensitivity may reflect properties of the underlying regulatory structure. The sensitivity variable, **S**, measures how a state function F is sensitive to the variation in parameters (**p**). **S** is defined as $\mathbf{S} = \frac{\partial F}{\partial \mathbf{p}}$, and the normalized sensitivity is $\mathbf{S}_n = \frac{\mathbf{p}}{F}\mathbf{S} = \frac{\partial \ln F}{\partial \ln \mathbf{p}}$ (36). Here, we separately analyze the sensitivity of the period and amplitude of oscillations for different clock components to changes in a set of nine parameters.

On the one hand, each clock element has the same period length, which is most sensitive to the degradation rates of *frq* mRNA and FRQ, k_2 and k_4 (Fig. 3). This is consistent with Table 2. Therefore, the degradation processes play important roles in controlling the period length, consistent with the analysis in the Goodwin model (24). On the other hand, for different clock elements, the oscillation amplitudes are sensitive to distinct parameters. The oscillation amplitude of [WCC*] is most sensitive to K_1, i.e., the concentration of WCC* when the *frq* transcription rate is half the maximum. The oscillation amplitudes of [*frq*] and [FRQ] are more sensitive to the Hill coefficient n and the maximum rate constants of reversible phosphorylation, k_5 and k_6. In general, the period has a lower sensitivity than the amplitudes toward changes in the same parameters except k_2 and k_4. This suggests that the period is more robust than the amplitude in circadian rhythms, which ensures stable rhythmic outputs.

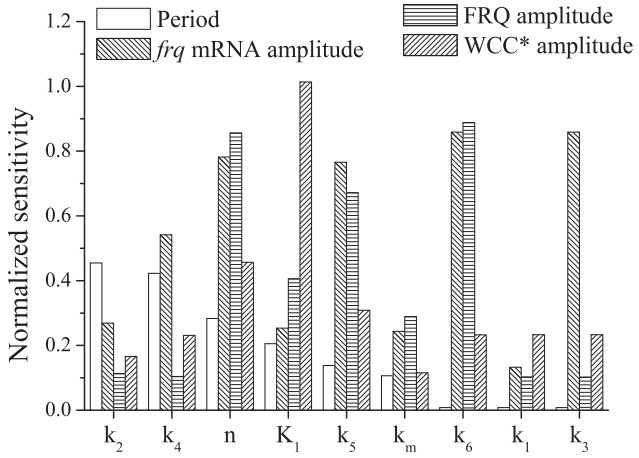

FIGURE 3 Parameter sensitivity analysis. The sensitivity of the period length to changes in parameter values is indicated by open bars, which are arranged on abscissa in descending order of sensitivity value. Also shown is the sensitivity of oscillation amplitudes to variations in the same parameters, which is characterized by the bars with distinct field patterns for different clock components.

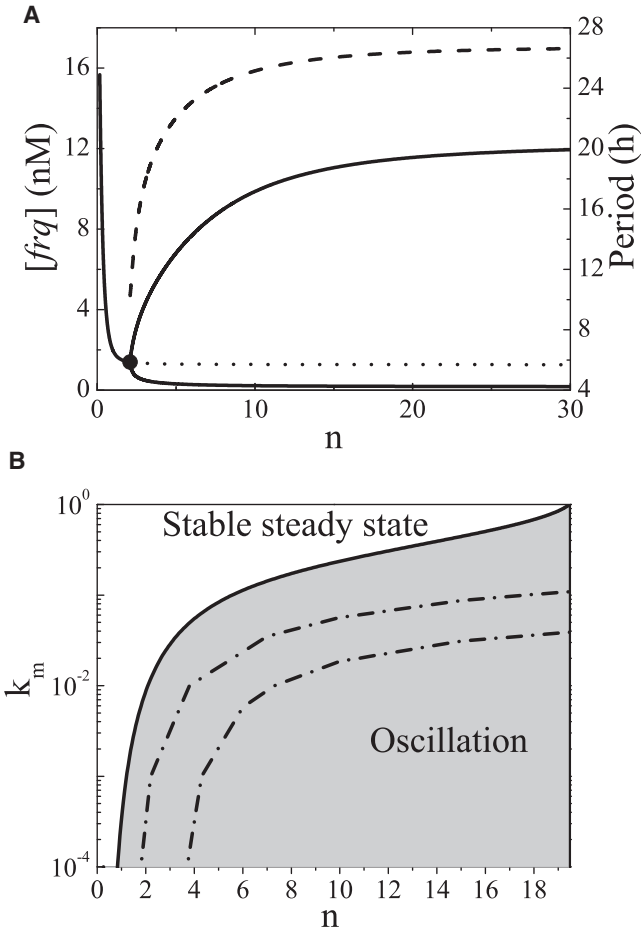

FIGURE 4 Dependence of circadian rhythms on the Hill coefficient n and the relative Michaelis constant k_m. (*A*) Bifurcation diagram of FRQ level as a function of n. When $n < 2$, the line shows its steady-state value; when $n \geq 2$, the two solid lines represent the maximum and minimum values of oscillations and the dashed line shows the corresponding period length, whereas the dotted line shows the unstable steady-state value. The Hopf bifurcation point is marked by the solid circle. (*B*) Two-parameter bifurcation diagram. The steady state is separated from the oscillatory state by the solid line. The region enclosed by two dash-dotted lines corresponds to the oscillations with the period length 20 ~ 24 h and the phase difference between the peak levels of *frq* mRNA and FRQ 4 ~ 6 h.

Dependence of circadian rhythms on n and k_m

Here, we explore the effects of the Hill coefficient n and the relative Michaelis constant k_m on circadian rhythms via bifurcation analysis. The value n characterizes the cooperativity of WCC proteins in binding to the *frq* promoter to activate its expression, while k_m quantifies the saturation degree of the reversible phosphorylation reactions. We first investigate the dependence of circadian oscillations on n (Fig. 4 *A*). Sustained oscillations are an emergent property of the model

system. When $n < 2$, the system evolves toward a stable steady state; when $n \geq 2$, the steady state becomes unstable and limit-cycle oscillations occur via Hopf bifurcation. The period length is between 20 and 24 h when $4 \leq n \leq 7$ (see *dashed line* in Fig. 4 *A*). When n becomes larger, both the period and the amplitude tend to be saturated, with their values separately approaching 27 h and 12 nM.

We then show the dependence of oscillations on both n and k_m (Fig. 4 *B*). On the one hand, the curve that separates the steady state from the oscillatory state has a positive slope, i.e., n and k_m are positively correlated. On the other hand, considering that the period length and phase lag should be within the physiological ranges, the values of k_m and n are constrained within an appropriate regime, which is enclosed by two dash-dotted curves. Clearly, k_m should be smaller than 0.1 when $n < 18$. However, as k_m is further reduced, the width between the two curves becomes narrow, and thus a tradeoff may lead to an optimal value of k_m, such as $k_m = 0.01$, where n can take a value between 4 and 7. The small k_m means that the enzymes involved in reversible phosphorylation are limited and the enzyme level is lower than the substrate level; consequently, both the kinase and the phosphatase are saturated by their substrates. Therefore, our model can bypass the requirement of high Hill coefficient for circadian oscillations when the enzymes operate near saturation.

It is worth comparing our model with the three-variable Goodwin model (37). The essential difference between the two models is that reversible phosphorylation of WCC is considered here. In the Goodwin model, large n ($n > 8$) is required for generating oscillations (38); but here only $n \geq 2$ is needed for oscillations with the standard parameter set. Moreover, the oscillation can be generated without any cooperativity in our model; for example, that occurs in the case of $n = 1$ and $k_m = 10^{-4}$ (see Fig. 4 *B*). These indicate that the phosphorylation process can generate sensitivity equivalent to strong cooperativity with a large coefficient, facilitating the occurrence of oscillations.

Role of phosphorylation in generating robust circadian oscillation

A key consequence of small k_m is the presence of a threshold for sharply inactivating WCC by FRQ (*black line* in Fig. 5 *A*). When k_m is sufficiently small, the enzymes for the phosphorylation and dephosphorylation reactions work near saturation, and thus the reactions operate at rates independent of the amounts of substrates (Fig. 5 *B*). The steady-state value of [WCC*] depends on the maximum reaction rates, i.e., k_5 and k_6[FRQ]. If $k_5 > k_6$[FRQ], most WCC proteins are in the hypophosphorylated state; otherwise, most WCC proteins are in the hyperphosphorylated state. That is, [WCC*] behaves like a switch and there exists a threshold of [FRQ], i.e., $[FRQ]_{th} = k_5/k_6$ (point *c* in Fig. 5, *A* and *B*). [WCC*] is close to $[WCC]_t$ when [FRQ] is below the threshold and is close to 0 otherwise. The steepness of this change depends remarkably on k_m. Indeed, a small change in [FRQ] around $[FRQ]_{th}$ can alter the steady state of [WCC*] dramatically from one extreme to the other (see points *a* and *b* in Fig. 5, *A* and *B*). Therefore, WCC* level is ultrasensitive to such a change in FRQ level, and this creates a molecular switch controlled by FRQ. The phenomenon described above is termed zero-order ultrasensitivity,

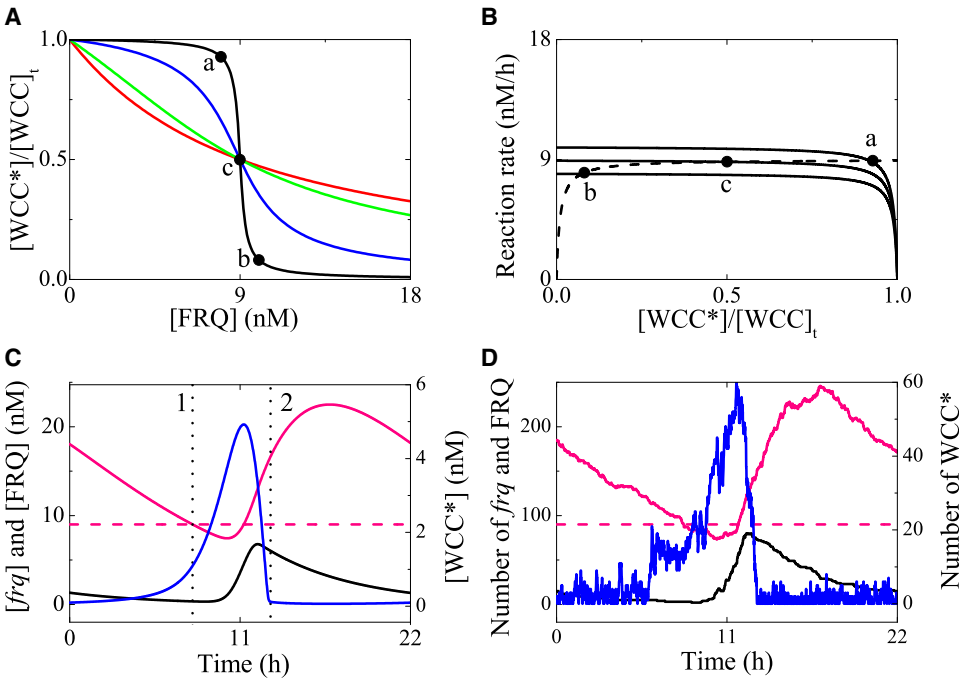

FIGURE 5 Effects induced by zero-order ultrasensitivity. (*A*) Fraction of active WCC in the steady state as a function of FRQ level for different relative Michaelis constants: $k_m = 0.01$ (*black*), 0.1 (*blue*), 1 (*green*), or 10 (*red*) (color online only). (*B*) Reaction rates for reversible phosphorylation of WCC*. Solid lines represent the phosphorylation rate for different concentrations of FRQ level (8, 9, and 10 nM, from *top* to *bottom*); dashed line describes the dephosphorylation rate, which is independent of FRQ level. The marked points correspond to the steady states in panel *A*. The oscillations of *frq* mRNA (*black*), FRQ (*pink*), and WCC* (*blue*) levels during one circadian cycle in the absence (*C*) or presence of noise (with $\Omega = 10$) (*D*). Pink dashed lines represent the threshold value of FRQ level. The dotted line 1 denotes the time when FRQ level crosses the threshold from above, whereas line 2 denotes the time when WCC* level crosses a small value such as 0.1 from above.

which was first reported decades ago (39) and verified experimentally in several enzymatic systems controlled by covalent modification, such as isocitrate dehydrogenase (40) and glycogen phosphorylase (41). Therefore, in our model, FRQ is indeed able to efficiently suppress the activity of WCC via the phosphorylation effect.

When k_m becomes larger, the transition curve of [WCC*] versus [FRQ] becomes more smooth and finally presents a hyperbolic nature without ultrasensitivity (Fig. 5 *A*). Under those conditions, large n is needed to produce oscillations as shown in Fig. 4 *B*. Note that the above analysis is based on the steady-state level of WCC* as a function of [FRQ]; such analysis provides an approximation of the relationship between [WCC*] and [FRQ] because the reversible phosphorylation processes are much faster than other processes.

That the activity of WCC is efficiently regulated by FRQ in a switchlike manner has advantages in generating robust circadian rhythms. First, it plays an essential role in lengthening the time delay in the negative feedback, thereby facilitating oscillations as shown above. Only when [FRQ] approaches the threshold from below, WCC is inhibited. Consequently, an intrinsic time delay is generated (not extrinsically added to the rate equations). Therefore, this effect effectively loosens the requirement for strong cooperativity in transcriptional activation for sustained oscillation.

Second, the oscillation of [WCC*] is spiky, which makes the oscillator robust to intrinsic noise. During one circadian cycle, the activation of WCC is restricted within a short time interval lasting ~5 h (see the range between the *dotted lines* 1 and 2 in Fig. 5 *C*). [WCC*] rises evidently after [FRQ] drops below the threshold but quickly decreases when [FRQ] rises above the threshold. Beyond this regime, WCC is almost suppressed and the concentration of WCC* is at a low level. This leads to the pulselike oscillations of [WCC*].

Indeed, the presence of the threshold in inactivating WCC functions like a barrier against noise-induced activation of WCC (Fig. 5 *D*). During one circadian cycle, for example, the amount of WCC* is fast accumulated to fire a pulse within the temporal interval where FRQ level is below the threshold. Far from that interval, the amount of WCC* is at a low level and small fluctuations in FRQ amount cannot trigger a pulse in WCC* amount. Meanwhile, since the *frq* transcription is induced by WCC*, no remarkable fluctuations occur in the number of *frq* mRNA. Consequently, the rhythmicity is kept even at high noise levels. It is worth noting that the previous model with interlinked positive and negative feedback also proposed a mechanism that suppresses noise-evoked fluctuations based on threshold crossing (42). In that case, however, the threshold is generated owing to the positive feedback.

Last, we systematically explore the robustness of circadian rhythm to molecular noise. Fig. 6, *A–C*, display the temporal evolution of the numbers of *frq* mRNA and FRQ molecules. Varying the value of Ω, we can get different noise intensity, which is generally proportional to $1\sqrt{\Omega}$. As the noise strength is increased, the oscillation amplitudes are more variable. Fig. 6, *D–F*, show the corresponding power spectrum of FRQ amount. Several aspects are worth noting. First, for large Ω (say $\Omega = 100$), there exists a high peak and the peak frequency is close to that in the deterministic system ($1/22.03 \sim 0.0454\ h^{-1}$). This indicates that the rhythmicity is maintained in the presence of noise. Second, as Ω decreases, the main peak becomes short and wide, indicating that the noise is strengthened to undermine the rhythmicity. Third, under the extreme condition, say $\Omega = 1$, although the number of *frq* mRNA is even <10, a bump is still visible in the spectrum, suggesting that the rhythmicity is not totally buried in the noise. Thus, the circadian oscillations presented here are generally robust to molecular noise.

SUMMARY AND DISCUSSION

In this article, we constructed a minimal model for the *N. crassa* circadian clock and identified the critical roles of reversible phosphorylation in generating robust circadian rhythms. We found that the activity of WCC can be repressed by FRQ in a switchlike manner owing to zero-order ultrasensitivity. This effect facilitates the generation of circadian oscillations and drives the spiky oscillation in the level of active WCC, which makes the clock robust to molecular noise. Thus, our results suggest that the phosphorylation of clock elements plays critical roles in circadian clocks.

One important role of reversible phosphorylation of WCC is the generation of the threshold for inactivating WCC based on the zero-order ultrasensitivity mechanism. Zero-order ultrasensitivity was reported decades ago and was shown to be important for producing all-or-none phenomena in cell signaling (43). It was also suggested to play a critical role in generating cell cycle oscillation (44). However, to our knowledge, it has never been studied in the context of circadian clocks. On the other hand, the condition for generating the threshold is the saturation of enzymatic reactions, which prevails in the models for circadian clocks (23) and has been shown in other biochemical reactions (40,41). It would be intriguing to experimentally measure the Michaels constants and explore the zero-order sensitivity in circadian clocks.

Robustness is an important property of biological functions. For the models of circadian clock, robustness is even considered as a criterion (45). Previously, a hysteresis-based mechanism was proposed for circadian clocks (42,45). By interlinking positive and negative feedback loops between clock elements, a kind of relaxation oscillation can be generated. The positive feedback alone creates a bistable switch for the level of the positive element, with its status depending on the level of the negative element. The slow rise and fall in the level of the negative element causes the level of the positive element to repeatedly alternate between the two states. This kind of oscillation is robust to molecular noise (42,45). Specifically, even when the time-averaged number

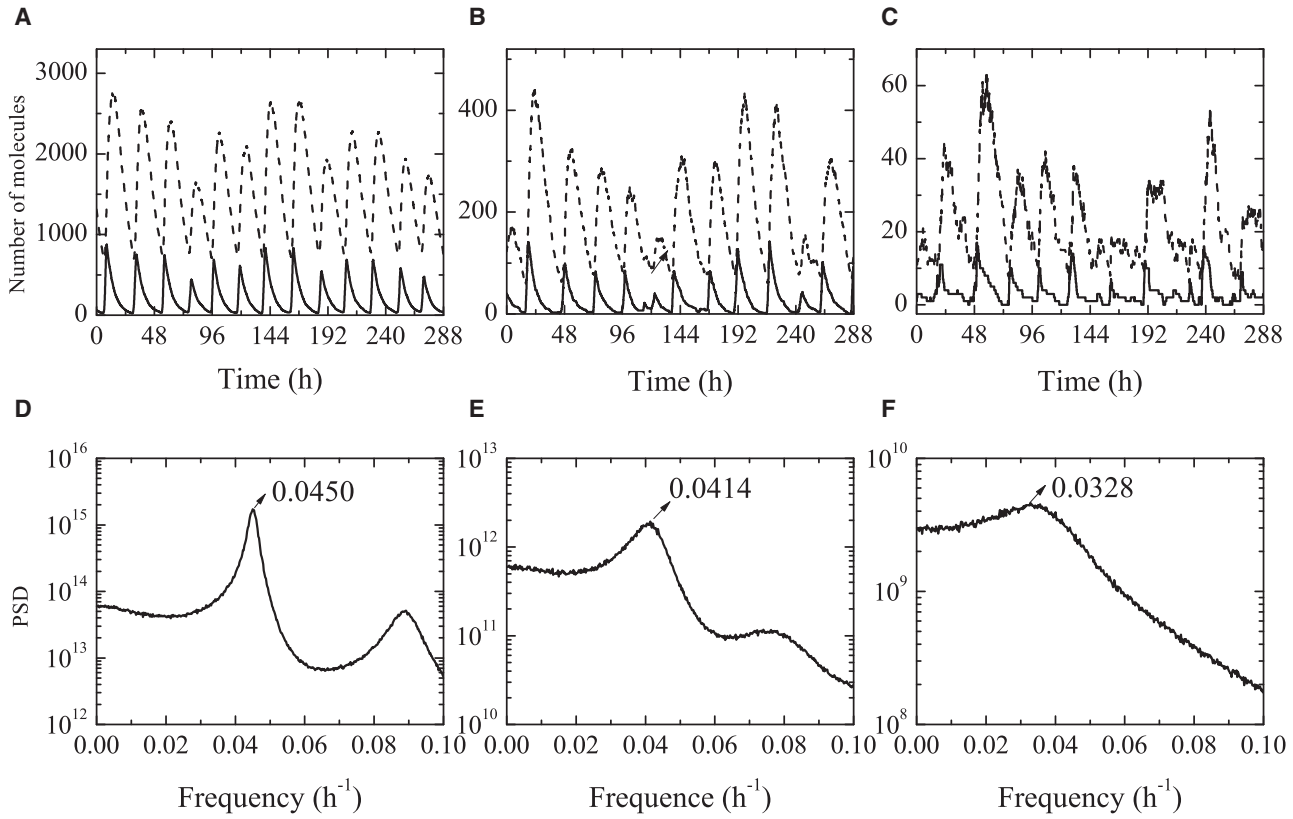

FIGURE 6 Robustness of circadian oscillations to molecular noise. (*A–C*) Oscillations of the amounts of *frq* mRNA (*solid lines*) and FRQ (*dashed lines*) with different Ω: 100 (*A*), 10 (*B*), and 1 (*C*). (*D–F*) The power spectrum density (*PSD*) of FRQ amount corresponding to the above panels. The peak frequency is marked in the panels, and the corresponding period is 22.22 h (*D*), 24.15 h (*E*), and 30.49 h (*F*), respectively.

of mRNA molecules is <1, the oscillation of protein levels can still be present (42). This is also the case in our model; the rhythm still exists when the number of *frq* mRNA is <10. The present oscillator can also be considered as a kind of relaxation oscillator. However, the switch is created by reversible phosphorylation and the positive feedback seems unnecessary. That is, the core negative feedback loop is able to generate robust circadian oscillations (46).

The spiky oscillations are often related to some kinds of functions. For example, the spiky oscillation of NF-κB level provides cells with high sensitivity to changes in input signals (29). Here, the spiky oscillation of the activated WCC may subserve controlling circadian outputs. In *N. crassa*, WCC* binds to the C-box of clock-controlled genes (ccgs), inducing their transcription. Some ccgs encode transcription factors, which further regulate the expression of other ccgs. Thus, a hierarchical organization for circadian output is formed (47,48). The *Z* values for oscillations of elements decrease along this signaling pathway. Thus, the spiky oscillation of [WCC*] with large *Z* is more likely to induce oscillations in the products of ccgs with a wide distribution of *Z* values (i.e., multiple oscillating shapes). This will ensure a wide variety of rhythmic activities in physiology and behavior.

Recently, there is growing interest in exploring the effects of reversible phosphorylation in circadian clocks (13). For example, more phosphorylation sites of WCC were identified in *N. crassa* (49). Here, our model also focuses on the role of reversible phosphorylation in closing the negative feedback loop, which is largely different from the previous models (14,15,50). Our results not only can reproduce the circadian rhythm in the wild-type frq^{+} strain, but also can be consistent with the experimental observations in *frq* mutant strains. Specifically, our model also reveals the effects of phosphatase mutation on circadian rhythms, which are in agreement with experimental observations. This is absent in the previous models.

Moreover, it is worthy to compare our work with that by Hong et al. (51). It was shown (51) that a small amount of FRQ can inhibit a large amount of WCC in the nucleus via 1:1 noncatalytic stoichiometric binding in the absence of phosphorylation of WCC, provided there is FRQ-dependent clearance of WCC from the nucleus. The nuclear clearance of WCC corresponds to either the degradation of WCC or the export of WCC to the cytoplasm. However, it was experimentally shown that the transactivity of WCC cannot be inhibited without FRQ-promoted phosphorylation of WCC. For example, it was reported that hypophosphorylated WCC can bind to the *frq* promoter even in the presence of FRQ, whereas the binding of hyperphosphorylated WCC to the promoter is compromised even when FRQ is depleted

(16). Moreover, when the kinase activity of CKI/II is reduced or undermined by mutation, even a large amount of FRQ cannot inhibit WCC (17). Clearly, these aspects cannot be explained by only considering direct binding of FRQ to WCC. Differently, our model was constructed based on the FRQ-dependent phosphorylation of WCC, and the results are consistent with the experimental observations. Nevertheless, it is quite possible that the phosphorylation of WCC requires that FRQ first binds to WCC. In fact, the phosphorylation process described by the Michaelis-Menten function involves two steps: FRQ first binds to WCC via 1:1 stoichiometry, and then CKI or CKII is recruited by FRQ (or is already in complex with FRQ) to phosphorylate WCC and inhibit it (17,52). After that, FRQ is disassociated from the inactive WCC.

On the other hand, Hong et al. found that with the phosphorylation of WCC involved, the phase difference between FRQ and WCC levels is too small compared with experimental measurements (51). Thus, they excluded the FRQ-dependent phosphorylation mechanism. In contrast, preliminary results show that the phase difference can be consistent with the experimental observation in our extended model with the total WCC level varying temporally. We think that the absence of dephosphorylation of WCC might be the reason for the inconsistence in Hong et al. (51). Taken together, we conclude that reversible phosphorylation of WCC is important for generating circadian clocks.

We have demonstrated that the ultrasensitivity in reversible phosphorylation is important for maintaining robust circadian rhythms. This may be a common mechanism for enhancing the robustness of circadian clocks; for example, the activity of the positive element CLOCK:BMAL1 in mammalian circadian systems is also regulated by its phosphorylation status (53). It would be intriguing to justify the presence of ultrasensitivity by experimentally measuring the response curve of the fraction of hypophosphorylated WCC versus FRQ level (like the *curves* in Fig. 5 *A*) using a frq^9*qa-2pfrq* strain (9,28). The strain is constructed in two steps. First, an integrated plasmid is made, with a *Neurospora qa-2* promoter fused in frame with *frq* open reading frame. Then, the plasmid is transformed into the lose-of-function mutant frq^9. Because the FRQ^9 is null-functional and FRQ expression is controlled by the promoter *qa-2p*, which is induced by the quinic acid (QA), the negative feedback between FRQ and WCC is undermined. That is, FRQ cannot inhibit its own expression. Consequently, the overt rhythmicity is absent regardless of the induced QA level (9). By adding different amounts of QA to the cultures of frq^9*qa-2pfrq*, distinct levels of FRQ can be induced. Because FRQ regulates the phosphorylation status of WCC, the level of hypophosphorylated WCC can be measured. In such a way, it is easy to check whether the ultrasensitivity effect exists.

Our model is designed to understand the essential role of FRQ-dependent phosphorylation of WCC in circadian oscillations, and thus only a minimal model is constructed. To investigate how a small amount of FRQ inactivates a large amount of WCC in the nucleus, a two-compartment model including the cytoplasmic and nuclear forms of clock elements may be required. Nevertheless, our work still provides insights into how that can happen. In the nucleus, the threshold value of [FRQ] for inactivating WCC can be small enough, so that even a small amount of FRQ can efficiently control the activity of a large pool of WCC. Moreover, it is easy to extend our model to include the positive feedback loop.

This work was supported by the National Natural Science Foundation of China (grant No. 10604028), the National Basic Research Program of China (grant No. 2007CB814806), the Natural Science Foundation of Jiangsu Province (grant No. SBK200910089), the Program for New Century Excellent Talents in University (grant No. 08-0269), and the Scientific Research Foundation for the Returned Overseas Chinese Scholars, State Education Ministry.

REFERENCES

1. Dunlap, J. C. 1999. Molecular bases for circadian clocks. *Cell*. 96: 271–290.
2. Reppert, S. M., and D. R. Weaver. 2002. Coordination of circadian timing in mammals. *Nature*. 418:935–941.
3. Young, M. W., and S. A. Kay. 2001. Time zones: a comparative genetics of circadian clocks. *Nat. Rev. Genet*. 2:702–715.
4. Dunlap, J. C. 2006. Proteins in the *Neurospora* circadian clockworks. *J. Biol. Chem*. 281:28489–28493.
5. Heintzen, C., and Y. Liu. 2007. The *Neurospora crassa* circadian clock. *Adv. Genet*. 58:25–66.
6. Brunner, M., and K. Káldi. 2008. Interlocked feedback loops of the circadian clock of *Neurospora crassa*. *Mol. Microbiol*. 68:255–262.
7. Crosthwaite, S. K., J. C. Dunlap, and J. J. Loros. 1997. *Neurospora wc-1* and *wc-2*: transcription, photoresponses, and the origins of circadian rhythmicity. *Science*. 276:763–769.
8. Cheng, P., Y. Yang, K. H. Gardner, and Y. Liu. 2002. PAS domain-mediated WC-1/WC-2 interaction is essential for maintaining the steady-state level of WC-1 and the function of both proteins in circadian clock and light responses of *Neurospora*. *Mol. Cell. Biol*. 22: 517–524.
9. Aronson, B. D., K. A. Johnson, J. J. Loros, and J. C. Dunlap. 1994. Negative feedback defining a circadian clock: autoregulation of the clock gene *frequency*. *Science*. 263:1578–1584.
10. Cheng, P., Y. Yang, C. Heintzen, and Y. Liu. 2001. Coiled-coil domain-mediated FRQ-FRQ interaction is essential for its circadian clock function in *Neurospora*. *EMBO J*. 20:101–108.
11. Denault, D. L., J. J. Loros, and J. C. Dunlap. 2001. WC-2 mediates WC-1-FRQ interaction within the PAS protein-linked circadian feedback loop of *Neurospora*. *EMBO J*. 20:109–117.
12. Froehlich, A. C., J. J. Loros, and J. C. Dunlap. 2003. Rhythmic binding of a WHITE COLLAR-containing complex to the *frequency* promoter is inhibited by FREQUENCY. *Proc. Natl. Acad. Sci. USA*. 100:5914–5919.
13. Brunner, M., and T. Schafmeier. 2006. Transcriptional and post-transcriptional regulation of the circadian clock of cyanobacteria and *Neurospora*. *Genes Dev*. 20:1061–1074.
14. Smolen, P., D. A. Baxter, and J. H. Byrne. 2001. Modeling circadian oscillations with interlocking positive and negative feedback loops. *J. Neurosci*. 21:6644–6656.
15. Francois, P. 2005. A model for the *Neurospora* circadian clock. *Biophys. J*. 88:2369–2383.

16. Schafmeier, T., A. Haase, K. Káldi, J. Scholz, M. Fuchs, et al. 2005. Transcriptional feedback of *Neurospora* circadian clock gene by phosphorylation-dependent inactivation of its transcription factor. *Cell*. 122:235–246.

17. He, Q., J. Cha, Q. He, H.-C. Lee, Y. Yang, et al. 2006. CKI and CKII mediate the FREQUENCY-dependent phosphorylation of the WHITE COLLAR complex to close the *Neurospora* circadian negative feedback loop. *Genes Dev*. 20:2552–2565.

18. Gallego, M., and D. M. Virshup. 2007. Post-translational modifications regulate the ticking of the circadian clock. *Nat. Rev. Mol. Cell Biol*. 8:139–148.

19. Nakajima, M., K. Imai, H. Ito, T. Nishiwaki, Y. Murayama, et al. 2005. Reconstitution of circadian oscillation of cyanobacterial KaiC phosphorylation in vitro. *Science*. 308:414–415.

20. Tomita, J., M. Nakajima, T. Kondo, and H. Iwasaki. 2005. No transcription-translation feedback in circadian rhythm of KaiC phosphorylation. *Science*. 307:251–254.

21. Lee, K., J. J. Loros, and J. C. Dunlap. 2000. Interconnected feedback loops in the *Neurospora* circadian system. *Science*. 289:107–110.

22. Cheng, P., Y. H. Yang, and Y. Liu. 2001. Interlocked feedback loops contribute to the robustness of the *Neurospora* circadian clock. *Proc. Natl. Acad. Sci. USA*. 98:7408–7413.

23. Kurosawa, G., and Y. Iwasa. 2002. Saturation of enzyme kinetics in circadian clock models. *J. Biol. Rhythms*. 17:568–577.

24. Ruoff, P., M. Vinsjevik, C. Monnerjahn, and L. Rensing. 1999. The Goodwin oscillator: on the importance of degradation reactions in the circadian clock. *J. Biol. Rhythms*. 14:469–479.

25. Liu, Y., N. Y. Garceau, J. J. Loros, and J. C. Dunlap. 1997. Thermally regulated translational control of FRQ mediates aspects of temperature responses in the *Neurospora* circadian clock. *Cell*. 89:477–486.

26. Gillespie, D. 1977. Exact stochastic simulation of coupled chemical reactions. *J. Chem. Phys*. 81:2340–2361.

27. Garceau, N. Y., Y. Liu, J. J. Loros, and J. C. Dunlap. 1997. Alternative initiation of translation and time-specific phosphorylation yield multiple forms of the essential clock protein FREQUENCY. *Cell*. 89:469–476.

28. Merrow, M. W., N. Y. Garceau, and J. C. Dunlap. 1997. Dissection of a circadian oscillation into discrete domains. *Proc. Natl. Acad. Sci. USA*. 94:3877–3882.

29. Krishna, S., M. H. Jensen, and K. Sneppen. 2006. Minimal model of spiky oscillations in NF-κB signaling. *Proc. Natl. Acad. Sci. USA*. 103:10840–10845.

30. Crosthwaite, S. K., J. J. Loros, and J. C. Dunlap. 1995. Light-induced resetting of a circadian clock is mediated by a rapid increase in *frequency* transcript. *Cell*. 81:1003–1012.

31. Leloup, J., D. Gonze, and A. Goldbeter. 1999. Limit cycle models for circadian rhythms based on transcriptional regulation in *Drosophila* and *Neurospora*. *J. Biol. Rhythms*. 14:433–448.

32. Aronson, B. D., K. A. Johnson, and J. C. Dunlap. 1994. Circadian clock locus *frequency*: protein encoded by a single open reading frame defines period length and temperature compensation. *Proc. Natl. Acad. Sci. USA*. 91:7683–7687.

33. Lakin-Thomas, P. L., and S. Brody. 2004. Circadian rhythms in microorganisms: new complexities. *Annu. Rev. Microbiol*. 58:489–519.

34. Yatzkan, E., and O. Yarden. 1999. The B regulatory subunit of protein phosphatase 2A is required for completion of macroconidiation and other developmental processes in *Neurospora crassa*. *Mol. Microbiol*. 31:197–209.

35. Yang, Y., Q. He, P. Cheng, P. Wrage, O. Yarden, et al. 2004. Distinct roles for PP1 and PP2A in the *Neurospora* circadian clock. *Genes Dev*. 18:255–260.

36. Stelling, J., E. D. Gilles, and F. J. Doyle. 2004. Robustness properties of circadian clock architectures. *Proc. Natl. Acad. Sci. USA*. 101:13210–13215.

37. Goodwin, B. C. 1965. Oscillatory behavior in enzymatic control processes. *Adv. Enzyme Regul*. 3:425–438.

38. Tyson, J. J., C. I. Hong, C. D. Thron, and B. Novak. 1999. A simple model of circadian rhythms based on dimerization and proteolysis of PER and TIM. *Biophys. J*. 77:2411–2417.

39. Goldbeter, A., and D. E. Koshland. 1981. An amplified sensitivity arising from covalent modification in biological systems. *Proc. Natl. Acad. Sci. USA*. 78:6840–6844.

40. LaPorte, D. C., and D. E. Koshland. 1983. Phosphorylation of isocitrate dehydrogenase as a demonstration of enhanced sensitivity in covalent regulation. *Nature*. 305:286–290.

41. Meinke, M. H., J. S. Bishop, and R. D. Edstrom. 1986. Zero-order ultrasensitivity in the regulation of glycogen phosphorylase. *Proc. Natl. Acad. Sci. USA*. 83:2865–2868.

42. Vilar, J. M. G., H. Y. Kueh, N. Barkai, and S. Leibler. 2002. Mechanisms of noise-resistance in genetic oscillators. *Proc. Natl. Acad. Sci. USA*. 99:5988–5992.

43. Tyson, J. J., K. C. Chen, and B. Novak. 2003. Sniffers, buzzers, toggles and blinkers: dynamics of regulatory and signaling pathways in the cell. *Curr. Opin. Cell Biol*. 15:221–231.

44. Goldbeter, A. 1991. A minimal cascade model for the mitotic oscillator involving cyclin and cdc2 kinase. *Proc. Natl. Acad. Sci. USA*. 88: 9107–9111.

45. Barkai, N., and S. Leibler. 2000. Circadian clocks limited by noise. *Nature*. 403:267–268.

46. Gonze, D., J. Halloy, and A. Goldbeter. 2002. Robustness of circadian rhythms with respect to molecular noise. *Proc. Natl. Acad. Sci. USA*. 99:673–678.

47. Vitalini, M. W., R. M. de Paula, W. D. Park, and D. Bell-Pedersen. 2006. The rhythms of life: circadian output pathways in *Neurospora*. *J. Biol. Rhythms*. 21:432–444.

48. Liu, Y., and D. Bell-Pedersen. 2006. Circadian rhythms in *Neurospora crassa* and other filamentous fungi. *Eukaryot. Cell*. 5:1184–1193.

49. Sancar, G., C. Sancar, M. Brunner, and T. Schafmeier. 2009. Activity of the circadian transcription factor White Collar Complex is modulated by phosphorylation of SP-motifs. *FEBS Lett*. 583:1833–1840.

50. Yu, Y. H., W. B. Dong, C. Altimus, X. J. Tang, J. Griffith, et al. 2007. A genetic network for the clock of *Neurospora crassa*. *Proc. Natl. Acad. Sci. USA*. 104:2809–2814.

51. Hong, C. I., I. W. Jolma, J. J. Loros, J. C. Dunlap, and P. Ruoff. 2008. Simulating dark expressions and interactions of *frq* and *wc-1* in the *Neurospora* circadian clock. *Biophys. J*. 94:1221–1232.

52. Gorl, M., M. Merrow, B. Huttner, J. Johnson, T. Roenneberg, et al. 2001. A PEST-like element in FREQUENCY determines the length of the circadian period in *Neurospora crassa*. *EMBO J*. 20:7074–7084.

53. Lee, C., J. P. Etchegaray, F. R. Cagampang, A. S. Loudon, and S. M. Reppert. 2001. Posttranslational mechanisms regulate the mammalian circadian clock. *Cell*. 107:855–867.